BIOMEDICAL REPORTS 24: 56, 2026

Preliminary exploration of the role of CD8+ T cells in anti-PD-1 antibody-induced myocarditis in C57BL/6 mice with Lewis lung carcinoma

HUACHUN CHEN[1], FAKAI LI[1], JUN SONG[1], SHENG WANG[2], HANWEN XU[1], RUOYA LYU[1], HUI ZHANG[3], GUIYUAN CHEN[4], XIAOYU WU[1] and MINGXING DING[5]

[1]Department of Respiratory and Critical Care Medicine, Jinhua Guangfu Tumor Hospital, Jinhua, Zhejiang 321001, P.R. China; [2]Department of Science and Education, Jinhua Guangfu Tumor Hospital, Jinhua, Zhejiang 321001, P.R. China; [3]Institute of Pharmacology, Jinhua Food and Drug Inspection and Testing Research Institute, Jinhua, Zhejiang 321002, P.R. China; [4]Nursing Faculty, Medical College of Jinhua University of Vocational Technology, Jinhua, Zhejiang 321007, P.R. China; [5]Medical Molecular Biology Laboratory, Medical College of Jinhua University of Vocational Technology, Jinhua, Zhejiang 321007, P.R. China

Received January 12, 2025; Accepted January 23, 2026

DOI: 10.3892/br.2026.2129

Abstract. Globally, ~33% of patients with non-small cell lung cancer receiving anti-PD-1 antibody therapy may experience significant immune-related adverse events (irAEs). Among these, myocarditis is a rare but lethal irAE. The aim of the present study was to preliminarily explore the role of $CD8^+$ T cells in anti-PD-1 antibody-induced myocarditis in C57BL/6 mice with Lewis lung carcinoma (LLC). Orthotopic transplantation models were established using wild-type or CD8 knockout ($CD8^{-/-}$) C57BL/6 mice. Wild-type and $CD8^{-/-}$ C57BL/6 mice were separately divided into three groups: Control, LLC and LLC + anti-PD-1. LLC cell suspensions ($1x10^5$ cells) with 50 μl Matrigel Matrix were orthotopically injected into the left lung lobe of wild-type or $CD8^{-/-}$ C57BL/6 mice. Following needle removal, the incision was sutured. At 10 days post-surgery, mice in the anti-PD-1 groups received an intraperitoneal injection of anti-PD-1 antibody (200 μg). After 3 weeks, all mice were humanely euthanized via intraperitoneal injection of sodium pentobarbital (200 mg/kg). The histopathological examination of tumor, lung and heart tissue was performed by Masson's trichrome and hematoxylin and eosin staining. Reverse transcription-quantitative PCR was carried out to determine the mRNA expression of monocyte chemotactic protein-1, interleukin-6, interferon-γ and tumor necrosis factor-α in myocardial tissue. Flow cytometry was used to analyze the ratio of $CD8^+$ and $CD4^+$ T cells and macrophages in myocardial tissues. Anti-PD-1 therapy effectively inhibited tumor growth and mitigated lung tissue damage. In wild-type C57BL/6 mouse, treatment with anti-PD-1 was associated with myocardial injury, inflammatory responses and a notable increase in the ratios of $CD8^+$ and $CD4^+$ T cells and macrophages. However, in $CD8^{-/-}$ C57BL/6 mice, no significant differences were observed in myocardial histopathology, inflammatory cytokine levels and the ratios of $CD4^+$ T cells and macrophages between the control, LLC and LLC + anti-PD-1 groups. Anti-PD-1 therapy did not cause significant damage to myocardial tissue. The presence of $CD8^+$ T cells facilitated the development of anti-PD-1-induced myocarditis by activating $CD4^+$ T cells, macrophages and inflammatory responses.

Correspondence to: Dr Xiaoyu Wu, Department of Respiratory and Critical Care Medicine, Jinhua Guangfu Tumor Hospital, 1296 Huancheng North Road, Jinhua, Zhejiang 321001, P.R. China
E-mail: 229901505@qq.com

Dr Mingxing Ding, Medical Molecular Biology Laboratory, Medical College of Jinhua University of Vocational Technology, 1188 Wuzhou Street, Wucheng, Jinhua, Zhejiang 321007, P.R. China
E-mail: dingmx@sina.com

Key words: immune checkpoint inhibitor, immune-related adverse event, Lewis lung carcinoma, anti-PD-1, myocarditis, $CD8^+$ T cell

Introduction

Lung cancer is a prevalent malignant tumor, with an incidence rate of 50.4/100,000 people in China in 2022 (1). Non-small cell lung cancer (NSCLC) accounts for ~85% of all lung cancer cases and has a 5-year survival rate of 18% (1). The treatment options for advanced NSCLC are limited, and targeted drugs are typically the first-line choice (2). In recent years, immune checkpoint inhibitors (ICIs) have facilitated a new era in tumor immunotherapy via blockade therapy (3). Clinical trials have demonstrated that the anti-programmed death 1 (PD-1) monoclonal antibody exhibits significant therapeutic efficacy in the treatment of numerous types of solid tumor, including NSCLC (4-6). However, certain patients receiving ICI treatment may experience significant side effects, known as immune-related adverse events (irAEs), which can damage different tissues or organs (7,8). In 2022, a multi-center study from China reported that among the various side effects, ICI associated-myocarditis is a rare yet lethal irAE, with an incidence of 1.14% and a mortality rate of 40-50% (9).

The symptoms of ICI associated-myocarditis are diverse, with the most common clinical manifestations including dyspnea, palpitations, chest pain and lower limb edema (10,11). Mild cases typically present with non-specific symptoms, such as general fatigue, nausea and discomfort, along with elevated cardiac biomarkers but without any specific symptoms (12). By contrast, severe cases may exhibit electrophysiological instability, fulminant myocarditis, hemodynamic instability, cardiogenic shock and death (13). Compared with other irAEs, ICI-associated myocarditis has a notably shorter onset time, with symptoms typically emerging ~34 days after the first dose of therapy (14,15). The typical pathological characteristics of ICI-associated myocarditis are focal or diffuse T cell infiltration, with $CD8^+$ T cell infiltration predominating in the majority of cases and $CD4^+$ T cells and macrophages being also prevalent (16). $CD8^+$ T cells induce myocardial injury via direct cytotoxic mechanisms, whereas $CD4^+$ T cells exacerbate the condition by modulating the inflammatory microenvironment and activating $CD8^+$ T cells (17). The dynamic balance and interaction between these cell types are crucial to the onset and progression of ICI-associated myocarditis. Anti-PD-1 therapy can interact with PD-L1, promoting the proliferation of $CD8^+$ T cells and enhancing their ability to kill cancer cells (18). However, anti-PD-1 not only blocks the negative regulatory signals of T cells to alleviate immune suppression and enhance their anti-tumor effects, but also intensifies normal immune responses, causing an imbalance in immune tolerance and giving rise to autoimmune-like inflammatory reactions in normal tissue (19). Therefore, investigating the role of $CD8^+$ T cells in the development of anti-PD-1-induced myocarditis during NSCLC treatment is key for improving the clinical management of ICI-associated myocarditis.

The present study aimed to elucidate the role of $CD8^+$ T cells in anti-PD-1 antibody-induced myocarditis in C57BL/6 mice with Lewis lung carcinoma (LLC).

Materials and methods

Cells, chemicals and antibodies. Mouse LLC cells (cat. no. CL-0140) were obtained from Procell Life Science and Technology. Matrigel Matrix was purchased from Corning, Inc. Glutamine, FBS, DMEM, streptomycin and penicillin were obtained from Gibco (Thermo Fisher Scientific, Inc.). DNase I, hyaluronidase and collagenase type V were obtained from Sigma-Aldrich (Merck KGaA). Masson's trichrome (cat. no. C0189S) and hematoxylin & eosin (HE) staining kit (cat. no. C0105S) were purchased from Beyotime Institute of Biotechnology. The total RNA Extraction kit (cat. no. LS1040) was acquired from Promega Corporation. First Strand (cat. no. 330421) and QuantiNova SYBR® Green PCR kits (cat. no. 208057) was obtained from Qiagen GmbH. The FITC anti-mouse CD4 antibody (cat. no. 100405), APC anti-mouse CD8a antibody (cat. no. 100711), Pacific Blue™ anti-mouse CD3 antibody (cat. no. 100213) and FITC anti-mouse CD68 antibody (cat. no. 137005; all 1:100) were obtained from BioLegend, Inc. Anti-PD-1 antibody was purchased from BD Biosciences.

Orthotopic transplantation model with LLC cells. LLC cells were cultured in DMEM supplemented with glutamine (2 mM), streptomycin/penicillin (1%) and FBS (10%) with 5% CO_2 at 37˚C. A total of 24 wild-type C57BL/6 male mice (age, 6-8 weeks; weight, 18-22 g) were purchased from Vital River Laboratories. A total of 18 CD8 knockout ($CD8^{-/-}$) C57BL/6 male mice (age, 6-8 weeks; weight, 18-22 g) were obtained from Jackson Laboratories. The genotype of the wild-type and $CD8^{-/-}$ mice was confirmed through PCR and agarose gel electrophoresis (Fig. S1; Data S1).

All mice were housed in specific pathogen-free environments with a temperature of 22±2˚C and a humidity of 50-60% and a 12 h light-dark cycle. The mice had unrestricted access to food and water. Following acclimatization, wild-type C57BL/6 mice were randomly divided into four groups (n=6/group) as follows: Control (sham-operated group), wild-type + anti-PD-1, wild-type LLC and wild-type LLC + anti-PD-1. $CD8^{-/-}$ mice were randomly separated into $CD8^{-/-}$ control, $CD8^{-/-}$ LLC and $CD8^{-/-}$ LLC + anti-PD-1 groups. The orthotopic transplantation model with LLC cells was established as previously described (20). Following anesthesia (50 mg/kg pentobarbital sodium), the mouse was positioned on the operating table and the thoracic cavity was exposed until the lung lobes were visible. Subsequently, LLC cell suspension ($1x10^5$ cells) containing 50 μl Matrigel Matrix was injected orthotopically into the left lobe of the lung. After removing the needle, the incision was sutured. A total of 10 days after surgery, mice in anti-PD-1 groups were administered anti-PD-1 antibody (200 μg) via intraperitoneal injection. The control mice underwent the same surgery and were administered 50 μl Matrigel Matrix or PBS vehicle on the same schedule. Animal health and behavior were monitored each day. A decrease in normal body weight >20% was defined as a humane endpoint; none of the mice reached the humane endpoint. After 3 weeks, all mice were humanely euthanized via intraperitoneal injection of 200 mg/kg sodium pentobarbital. Tumor, left lung and heart tissue were collected. The investigators were blinded to group identity. The present study was performed in accordance with the National Institutes of Health Guide for the Care and Use of Laboratory Animals (8th edition) (21). The experimental protocols were approved by the Experimental Animal Ethics Committee of Jinhua Food and Drug Inspection and Testing Research Institute (Jinhua, China; approval no. AL-JSYJ202023).

Histology. The tumor, left lung and left ventricle tissue were fixed (4% paraformaldehyde at 25˚C for 12 h), dehydrated and embedded in paraffin. Tissue samples were precisely sliced into sections measuring 4 μm in thickness. Following dewaxing and rehydration, sections were subjected to HE (hematoxylin for 5 min and eosin for 2 min at room temperature) and Masson's trichrome staining (Wiegert's iron hematoxylin for 8 min, Biebrich scarlet for 5 min and aniline blue for 5 min at room temperature). High-resolution images were captured using an OLYMPUS BX53 light microscope (n=9 fields of view/mouse) and analyzed using ImageJ version 1.54 (National Institutes of Health).

Flow cytometry. Heart tissue was dissected into small fragments (2 mm^3) and subjected to enzymatic digestion in DMEM enriched with DNase I (0.015 mg/ml), hyaluronidase

(0.2 mg/ml) and collagenase type V (0.5 mg/ml) for a duration of 2 h at 37˚C. Cell suspensions were prepared by passing the tissues through a 70-μm cell strainer. The single-cell suspensions were stained with Pacific Blue™ anti-mouse CD3, FITC anti-mouse CD4, APC anti-mouse CD8a and FITC anti-mouse CD68 antibody. Following 30 min incubation in the dark at 4˚C, the cells were washed three times with PBS, resuspended in PBS containing 1% FBS and analyzed using a FACScan flow cytometer (BD Biosciences). Flow cytometric data were analyzed using FlowJo software (version 10.8.1; BD Biosciences).

Reverse transcription-quantitative PCR. A total RNA extraction kit was used to extract the total RNA from left ventricle tissue. According to the manufacturer's protocol, RNA was used to produce cDNA using the First Strand Kit, followed by PCR analysis using a QuantiNova SYBR® Green PCR kit. The thermocycling conditions were as follows: 95˚C for 5 min, followed by 40 cycles of denaturation at 95˚C for 15 sec and annealing and extension at 60˚C for 40 sec. Gene expression was assessed using the $2^{-\Delta\Delta Cq}$ method (22), with GAPDH serving as a normalization control. Primer sequences are listed in Table I.

Statistical analysis. Each experiment was performed in triplicate. All data were analyzed with SPSS 23.0 statistical software (IBM Corp.) and presented as the mean ± standard deviation. One-way ANOVA followed by Tukey's post hoc test was used for data comparison. P<0.05 was considered to indicate a statistically significant difference.

Results

Anti-PD-1 therapy improves the histopathology of lung and tumor tissue but induces myocarditis in wild-type mice. HE staining was utilized to investigate the histopathological characteristics of tumor, lung and heart tissue (Fig. 1A and B). Tumor cells exhibited an increase in size, accompanied by a minor degree of hemorrhage and were organized in a sheet-like arrangement. Some cell nuclei showed an enlargement in volume, with an increased presence of mitotic figures. Inflammatory infiltration was evident within the interstitial space. Anti-PD-1 therapy inhibited tumor growth, as evidenced by a loose distribution of tumor cells and decreased numbers of mitotic figures. Hemorrhage was observed. The cellular distribution appeared uneven, with a small number of lymphocytes visible in the interstitial space. Infiltration of inflammatory cells was not prominent and vacuolar changes were evident in the cytoplasm. Compared with the control, LLC mice exhibited pronounced lung tissue damage characterized by disorganized and collapsed alveolar structures, extensive infiltration of inflammatory cells and interstitial congestion (the black arrow; Fig. 1C). These histopathological changes were mitigated by anti-PD-1 therapy (Fig. 1C). Morphology and structure of the myocardial tissue in the control group were normal (Fig. 1D). The myocardial fibers exhibited a neat arrangement, with clearly defined nuclei and no infiltration of inflammatory cells. Similar histopathology was observed in LLC mice. However, the intercellular spaces in the LLC + anti-PD-1 group were enlarged (the black arrow).

Table I. Primer sequences.

Gene	Sequence, 5'→3'
MCP-1	Forward: TGCCCTAAGGTCTTCAGCAC
	Reverse: AAGGCATCACAGTCCGAGTC
IL-6	Forward: GACAAAGCCAGAGTCCTTCAGA
	Reverse: TGTGACTCCAGCTTATCTCTTGG
IFN-γ	Forward: CGGCACAGTCATTGAAAGCC
	Reverse: TGCATCCTTTTTCGCCTTGC
TNF-α	Forward: TGCCACAAGCAGGAATGAGA
	Reverse: GACGTGGAAGTGGCAGAAGAG
GAPDH	Forward: CTGCACCACCAACTGCTTAG
	Reverse: GTCTGGGATGGAAATTGTGA

MCP-1, monocyte chemoattractant protein-1.

Additionally, there was infiltration of inflammatory cells (the red arrow). These results indicated notable impairment of myocardial tissue following treatment with anti-PD-1. In Masson's trichrome staining, red represents myocardial cells, while blue represents collagen fiber. Collagen fibers accounted for a relatively small proportion of healthy myocardial tissue. The proportion of collagen fibers in control and LLC mice groups was relatively small, however, LLC + anti-PD-1 group exhibited a significant increase in blue-stained area, characterized by extensive fibrotic tissue replacing normal myocardial tissue (Fig. 1E).

Anti-PD-1 therapy activates $CD8^+$ and $CD4^+$ T cells and macrophages and induces secretion of inflammatory cytokines in wild-type mice. Flow cytometry analysis indicated no significant differences in the ratios of $CD8^+$, $CD4^+$ and $CD68^+$ (macrophage marker) cells between the control and the LLC group (Fig. 2A). By contrast, anti-PD-1 therapy notably increased the percentages of $CD8^+$ and $CD4^+$ T cells and macrophages in myocardial tissue of LLC mice (Fig. 2A). Furthermore, the expression of inflammation-associated cytokines, including chemokine monocyte chemotactic protein-1 (MCP-1), IL-6, IFN-γ and tumor necrosis factor (TNF)-αwere significantly increased by anti-PD-1 (Fig. 2B).

Anti-PD-1 therapy improves the histopathology of tumor and lung tissue but does not induce significant myocardial injury in $CD8^{-/-}$ mice. After knocking out CD8 gene, tumor cells in LLC mice were arranged in a dense, sheet-like pattern, exhibiting notable proliferation and an increase in mitotic figures (Fig. 3A and B). The volume of the cell nucleus was enlarged, with meganuclei and multinucleated tumor cells present. Lymphocytes were found within the interstitial spaces. Following anti-PD-1 treatment, tumor cells exhibited a decrease in size and were arranged in loose pattern. There was also a notable decrease in mitotic figures along with moderate infiltration of inflammatory cells within the interstitium. No obvious pathological changes were observed in lung tissue of mice in the control or anti-PD-1 groups (Fig. 3C). Notably, the lung tissue of $CD8^{-/-}$ LLC mice was severely damaged, with

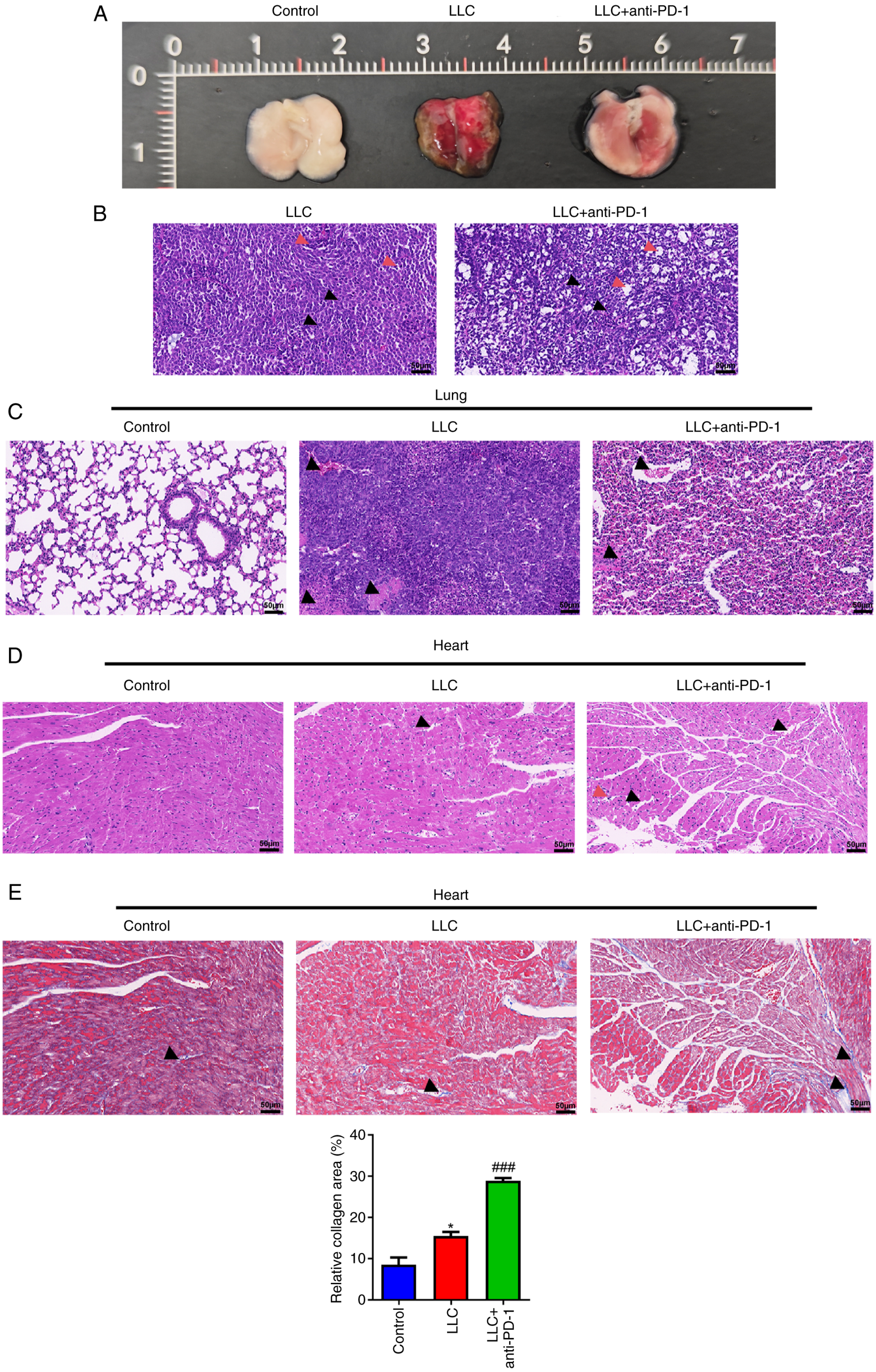

Figure 1. Anti-PD-1 therapy improves the histopathology of lung and tumor tissue but induces myocarditis in wild-type mice. (A) Representative photographs of the lungs containing the tumors. HE staining was performed to examine the histopathology of (B) tumor (black arrow, nucleus; red arrow, inflammatory cell infiltration), (C) lung (arrow, interstitial congestion) and (D) heart tissue (black arrow, intercellular space; red arrow, inflammatory cell infiltration). (E) Masson's trichrome staining was performed to examine the histopathology of heart tissue. Arrow, collagen fiber. Scale bar, 50 μm. *P<0.05 vs. control, ###P<0.001 vs. LLC. HE, hematoxylin-eosin; LLC, Lewis lung carcinoma.

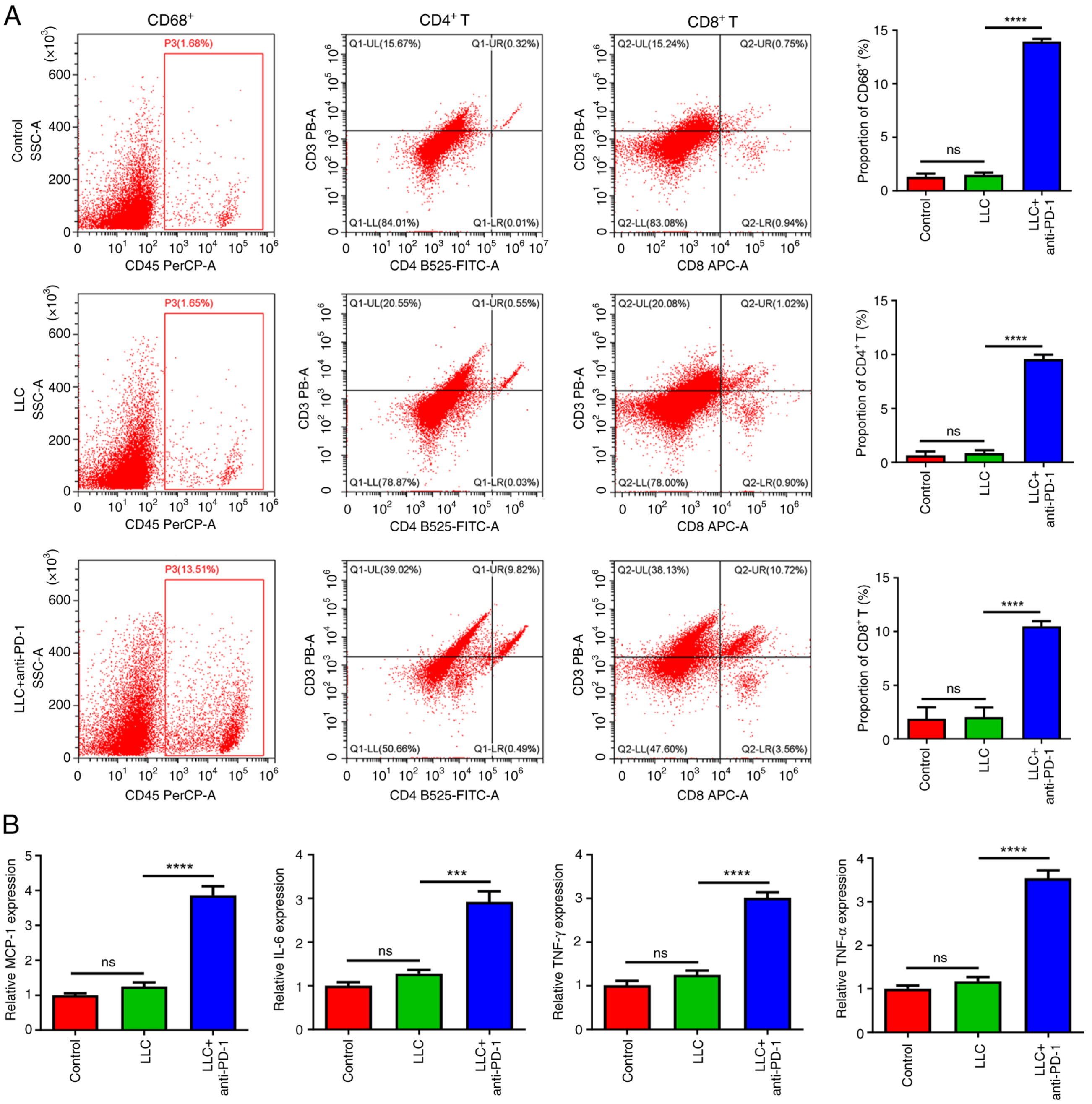

Figure 2. Anti-PD-1 therapy activates CD8+ and CD4+ T cells and macrophages and induces secretion of inflammatory cytokines in wild-type mice. (A) Ratios of CD68+, CD4+ and CD8+ T cells in myocardial tissue were analyzed through flow cytometry. (B) mRNA expression of MCP-1, IL-6, IFN-γ and TNF-α in myocardial tissue was determined by reverse transcription-quantitative PCR. ***P<0.001, ****P<0.0001. ns, not significant; MCP-1, monocyte chemoattractant protein-1; LLC, Lewis lung carcinoma.

notable inflammatory infiltration along with visible congestion and thickening of the lung interstitium. However, anti-PD-1 therapy alleviated pulmonary interstitial congestion and thickening. All groups exhibited normal morphology and structure of the myocardial tissue, with a well-organized arrangement of myocardial fibers, distinct cell nuclei and an absence of inflammatory cell infiltration (Fig. 3D). Notably, the intercellular space in $CD8^{-/-}$ LLC + anti-PD-1 group was observed to be slightly increased compared with the other groups (Fig. 3D). Masson's trichrome staining showed that a small amount of collagen fibers was observed in control, anti-PD-1 and LLC groups (Fig. 3E). By contrast, the $CD8^{-/-}$ LLC + anti-PD-1 group exhibited a significant increase in collagen fibers (Fig. 3E).

Anti-PD-1 therapy does not significantly alter $CD4^+$ T cell and macrophage levels or inflammatory cytokine secretion in $CD8^{-/-}$ mice. Ratios of $CD4^+$ T cells and macrophages in myocardial tissue were assessed. In $CD8^{-/-}$ mice, the ratio of $CD4^+$ T cells was significantly decreased compared with that of the wild-type mice (Fig. 4A). There were no significant differences between the other groups. Furthermore, expression of MCP-1, IL-6, IFN-γ and TNF-α was not significantly different between any groups (Fig. 4B).

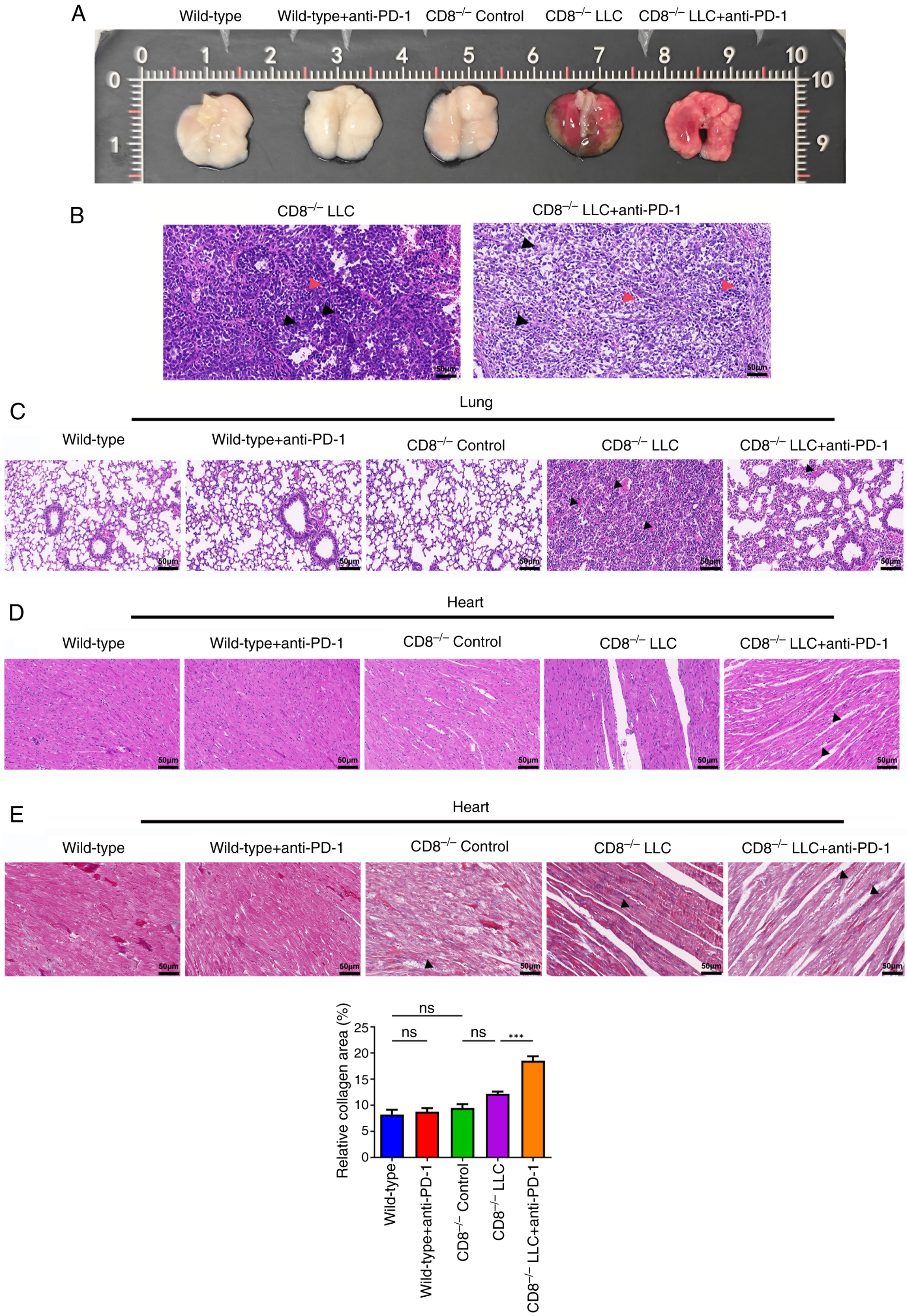

Figure 3. Effects of anti-PD-1 therapy on the histopathology of tumor, lung and heart tissue in CD8$^{-/-}$ mice. (A) Representative photographs of the lungs containing the tumors. HE staining was performed to examine the histopathology of (B) tumor (black arrow, nucleus; red arrow, inflammatory cell infiltration), (C) lung (arrow, interstitial congestion) and (D) heart tissue (black arrow, intercellular space; red arrow, inflammatory cell infiltration). (E) Masson's trichrome staining was performed to examine the histopathology of heart tissue. Arrow, collagen fiber. Scale bar, 50 μm. ***P<0.001. HE, hematoxylin-eosin; LLC, Lewis lung carcinoma; ns, not significant.

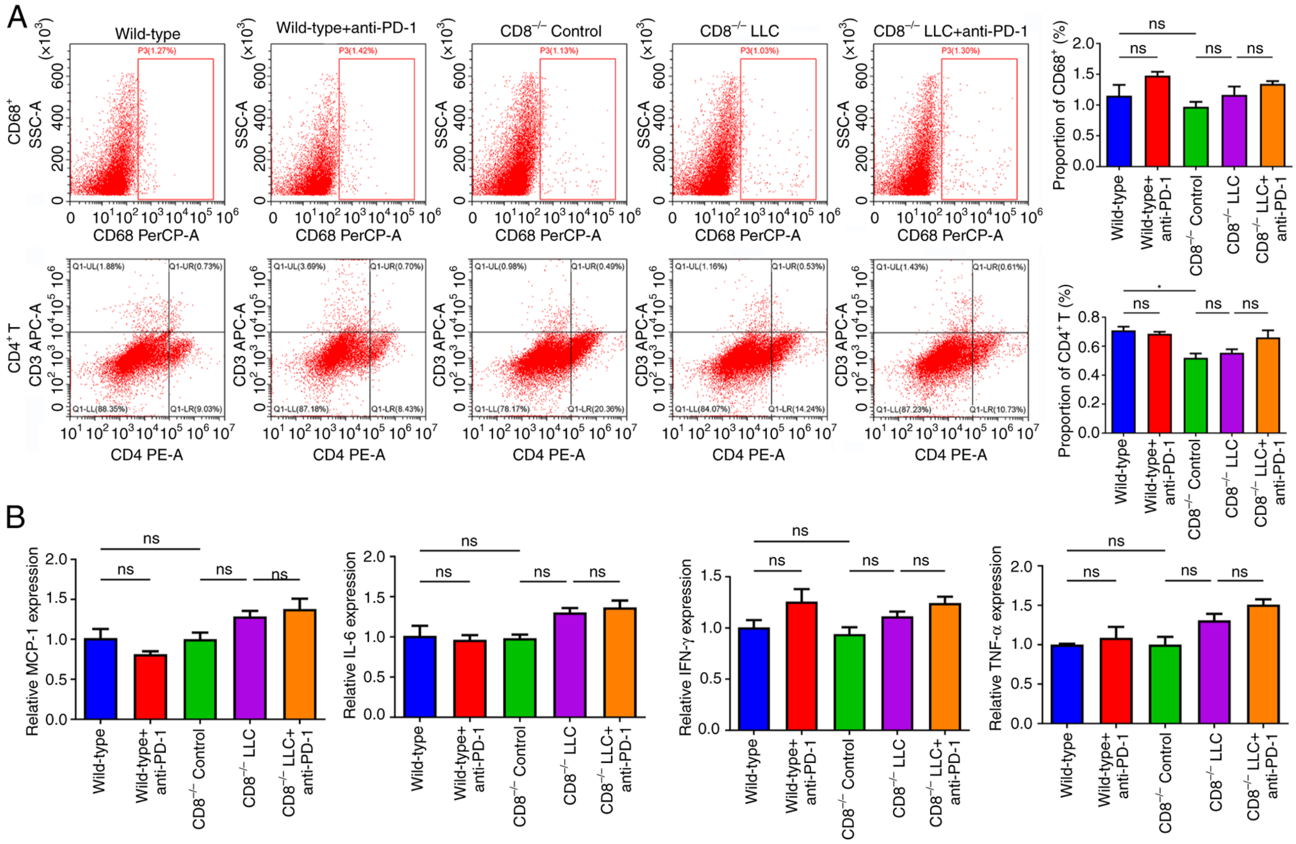

Figure 4. Effect of anti-PD-1 therapy on CD4+ T cell and macrophage levels and inflammatory cytokine expression. (A) Ratios of CD68+ and CD4+ T cells in myocardial tissue were analyzed through flow cytometry. (B) mRNA expression of MCP-1, IL-6, IFN-γ and TNF-α in myocardial tissue was determined via reverse transcription-quantitative PCR. *P<0.05. ns, not significant; LLC, Lewis lung carcinoma.

Discussion

Initially considered to be a rare irAE with an incidence rate ranging from 0.09 to 1.14%, recent studies have indicated that ICI-associated myocarditis has a high fatality rate (40-50%) (15,23). Al-Kindi and Oliveira (24) reported 250 cases of myocarditis associated with ICI. The aforementioned findings indicated increased reporting over time, with 18 cases documented between 2012 and 2015, followed by 70 cases in 2016 and 162 cases in 2017 (24). Therefore, while clinically significant myocarditis is uncommon, it should not be overlooked due to the rising number of patients with cancer undergoing ICI therapy. The present study established an orthotopic transplantation model with LLC cells. ICI associated-myocarditis required the presence of CD8+ T cells to activate CD4+ T cells and macrophages and induce inflammatory responses.

LLC cell line was isolated from the epidermoid carcinoma of the lung in mice. It is an essential tumor model in studies of therapeutic effects (25), vessel formation (26) and metastasis (27). LLC-bearing mice have been employed in experimental frameworks investigating NSCLC (28,29). The histopathological analysis revealed an increase in the presence of mitotic figures, along with pronounced infiltration of inflammatory cells within the tumor tissue. Concurrently, the structural integrity of lung tissue was compromised. These findings suggested that the orthotopic transplantation model was successfully established. Additionally, consistent with previous studies (5,30), anti-PD-1 therapy decreased nuclear division and infiltration of inflammatory cells and induced necrosis of tumor cells. Clinical observational studies have demonstrated that in patients with ICI associated-myocarditis, there is significant infiltration of inflammatory cells within the myocardial tissue and focal fibrosis is observed in some cases (31,32). In the present study, the histopathological examination of myocardial tissue revealed that the use of anti-PD-1 resulted in fibrosis and infiltration of inflammatory cells. In wild-type mice, levels of cytokines associated with inflammation, such as MCP-1, IL-6, IFN-γ, and TNF-α, were significantly elevated following anti-PD-1 treatment. These cytokines are associated with immune-mediated heart damage. Overactivated T cells and macrophages release notable amounts of MCP-1, thereby establishing a positive feedback loop of inflammation-chemotaxis that exacerbates myocardial injury (33). IL-6 is a crucial pro-inflammatory cytokine that can be secreted by T cells, macrophages and cardiomyocytes. It plays an integral role in the process of myocardial fibrosis (34). IFN-γ enhances the antigen presentation capacity of macrophages, promotes a T helper 1-type immune response and induces the expression of major histocompatibility complex (MHC)-I molecules in cardiomyocytes, rendering them susceptible to attack by CD8+ T cells (12). TNF-α, secreted by T cells, macrophages and cardiomyocytes, can directly induce myocardial cell apoptosis and inhibit myocardial contractility (34). Collectively, the present findings indicated that such treatment may damage the myocardium.

The heart is an organ with immune privilege, making immune reactions within it particularly hazardous, as they can result in life-threatening arrhythmia and severe heart failure (15). Its lack of regenerative ability, combined with a heightened risk of arrhythmia from minor injuries and rich blood supply, renders the heart susceptible to damage from the immune system (15). Histopathological examinations of samples from patients with ICI associated-myocarditis show a heightened presence of macrophages and T lymphocytes (including $CD8^+$ and $CD4^+$ types) within the myocardial tissue (12,35). Additionally, some reports have demonstrated that lung biopsy samples from patients with NSCLC who underwent anti-PD-1 therapy exhibit high infiltration of $CD8^+$ and $CD4^+$ T cells (36,37). These findings align with the abnormally elevated levels of $CD4^+$ and $CD8^+$ T cells and macrophages observed in patients with ICI-induced myocarditis (16,17). Modulation of immune checkpoints is a key mechanism for evading immune surveillance by inhibiting activated T cells (38). Antibodies that suppress PD-1 improve and restore the functionality of exhausted T cells and enhance their anti-tumor immune response (39). Therefore, it was hypothesized that the administration of anti-PD-1 therapy in lung cancer inhibits the PD-1 signaling pathway, thereby alleviating T cell suppression and enhancing the immune system capacity to target tumor cells. This process leads to the activation and proliferation of immune cells throughout the body, including $CD8^+$ T cells. Consequently, these activated immune cells may circulate systemically and infiltrate myocardial tissue, resulting in immune-mediated damage to cardiac structures. The present results corroborated previous research findings, demonstrating notably elevated ratios of $CD4^+$ and $CD8^+$ T cells and macrophages in the myocardial tissues of mice treated with anti-PD-1. By contrast, the number of these cells did not exhibit significant increases in the absence of anti-PD-1 treatment. In ICI-induced myocarditis, $CD4^+$ T cells play promote pathogenesis by regulating the inflammatory microenvironment and co-activating $CD8^+$ T cells (17). The present findings were consistent with the aforementioned study highlighting that $CD4^+$ T cells assist $CD8^+$ T cells in mediating the immunopathological process of this condition. As key antigen-presenting cells (APCs), macrophages (marked by CD68) contribute to myocarditis by secreting pro-inflammatory cytokines (40,41). The present study demonstrated that anti-PD-1 therapy elevated macrophage and cytokine levels in LLC mice. These results suggested that the cytokines established an inflammation-chemotaxis feedback loop to amplify myocardial damage and recruit $CD8^+$ T cells. Jiménez-Alejandre *et al* (16) noted dendritic cells (as potent APCs) present myocardial or cross-reactive tumor antigens via MHC molecules to prime $CD4^+$ T cells and enhance $CD8^+$ T cell activation. In the present study, anti-PD-1 did not alter $CD4^+$ T cell/macrophage infiltration or cytokine levels in $CD8^{-/-}$ LLC mice compared with the controls, indicating $CD4^+$ T cell activation and APC recruitment require $CD8^+$ T cells to initiate the pathogenic cascade of ICI-induced myocarditis. Anti-PD-1 therapy was effective in inhibiting tumor growth and ameliorating lung tissue damage. In the absence of CD8 gene, no significant differences were observed in myocardial histopathology or expression of MCP-1, IL-6, IFN-γ and TNF-α between groups. $CD8^{-/-}$ LLC + anti-PD-1 mice showed an increase in collagen fibers compared with $CD8^{-/-}$ LLC mice. These results indicated the key role of $CD8^+$ T cells in ICI associated-myocarditis. There were no significant differences in the ratios of $CD4^+$ T and macrophages between groups, which may indirectly suggest that the presence of $CD8^+$ T cells is a prerequisite for the activation of $CD4^+$ T cells and macrophages as well as subsequent inflammatory cell infiltration.

The present study confirmed anti-PD-1 can trigger myocardial inflammatory infiltration and fibrosis, consistent with the study conducted by Johnson *et al* (35) that reported focal/diffuse T cell infiltration and fibrosis in biopsy samples of patients with myocarditis. $CD8^+$ T cells serve as central pathogenic mediators, aligning with the previous studies emphasizing $CD8^+$ T cell cytotoxicity and depletion abolishing myocarditis (17,42). Furthermore, pro-inflammatory cytokines (MCP-1, IL-6, IFN-γ, TNF-α) and $CD68^+$ macrophages, key contributors to inflammation progression, were identified, consistent with findings on cytokine elevation and macrophage-mediated damage reported by Patel *et al* (43) and Wang *et al* (44). Additionally, the present study demonstrated that $CD8^+$ T cells serve as upstream initiators of $CD4^+$ T cell and macrophage activation and identified $CD8^+$ T cells as the common mediator linking anti-tumor activity and cardiac toxicity, whereas prior clinical studies have primarily focused on myocarditis incidence and prognostic markers (45,46).

The present findings suggest potential for advancements in clinical practice aimed at preventing or treating myocarditis via regulation of $CD8^+$ T cell activity. For example, activation of $CD8^+$ T cells depends on costimulatory molecules, such as CD28/B7 and CD137/CD137L (47). Blocking their interaction may inhibit the function of $CD8^+$ T cells. Activated $CD8^+$ T cells exhibit high levels of pro-apoptotic molecules, such as Fas. Inducing apoptosis of $CD8^+$ T cells may mitigate myocardial injury. Chimeric antigen receptor-$CD8^+$ T cells engineered to target tumor antigens can be designed to minimize the risk of non-specific myocardial damage. Regulation of the function and localization of $CD8^+$ T cells may prevent ICI-associated myocarditis and treat lung cancer. The CCL5-CCR5 axis is activated in myocarditis progression (48), whereas the tumor microenvironment predominantly uses the CXCL9/CXCL10-CXCR3 axis to recruit anti-tumor $CD8^+$ T cells (49). Consequently, CCR5 antagonists (such as maraviroc) can be employed in combination therapy to selectively inhibit the migration of self-reactive $CD8^+$ T cells to the heart without compromising the infiltration of $CD8^+$ T cells within tumors. Directly injecting anti-PD-1 antibodies into lung cancer lesions (pulmonary nodules) significantly enhances local drug concentration within tumors, achieving levels 10-100 times higher than those attained through systemic administration, while concurrently reducing peripheral blood drug concentrations and minimizing the effects of $CD8^+$ T cells on heart (50).

The present study had limitations. First, the specific mechanisms of $CD8^+$ T cells on the activation of $CD4^+$ T cells and macrophages are unknown. Further investigation into the role of $CD4^+$ T cells and macrophages in myocarditis is warranted. The sample size was relatively small, potentially leading to insufficient statistical power and an increased risk of false-negative or -positive results. Additionally, the present study did not exclude the potential effects of $CD8^{-/-}$ on other immune cells (such as natural killer and regulatory T cells) or molecular pathways other than the PD-1/PD-L1 pathway. For example, $CD8^{-/-}$ may alter the immune balance in the tumor microenvironment, however the present study did not measure associated markers (such as regulatory T cells and IL-10) to exclude confounding factors. Certain non-T cell-dependent mechanisms may be activated by anti-PD-1 treatment, and further investigation of regulatory T cell and PD-L1 expression levels is required.

In summary, the present study offers an initial investigation into the molecular mechanisms underlying $CD8^+$ T cell functions in anti-PD-1 antibody-induced myocarditis. Myocarditis induced by anti-PD-1 antibody required the involvement of $CD8^+$ T cells to activate both $CD4^+$ T cells and macrophages and stimulate inflammatory responses. These findings suggest inhibition of $CD8^+$ T cells can attenuate ICI-associated myocarditis, which may facilitate improved the treatment strategies for this condition.

Acknowledgements

Not applicable.

Funding

The present study was supported by The Science and Technology Project of Jinhua City in China (grant no. 2022-3-146).

Availability of data and materials

The data generated in the present study may be requested from the corresponding author.

Authors' contributions

MD and XW conceived and designed the study. HC, FL, JS, SW, HX, RL, HZ and GC analyzed and interpreted data. HC wrote the manuscript. MD and XW confirm the authenticity of all the raw data. All authors have read and approved the final manuscript.

Ethics approval and consent to participate

Experiments for animals were conducted in compliance with the National Institutes of Health Guide for the Care and Use of Laboratory Animals, and approved by the Experimental Animal Ethics Committee of Jinhua Food and Drug Inspection and Testing Research Institute (Jinhua, China; approval no. AL-JSYJ202023).

Patient consent for publication

Not applicable.

Competing interests

The authors declare that they have no competing interests.

References

1. Roller JF, Veeramachaneni NK and Zhang J: Exploring the Evolving scope of neoadjuvant immunotherapy in NSCLC. Cancers (Basel) 14: 741, 2022.
2. Li MSC, Mok KKS and Mok TSK: Developments in targeted therapy & immunotherapy-how non-small cell lung cancer management will change in the next decade: A narrative review. Ann Transl Med 30: 358, 2023.
3. Schoenfeld AJ, Lee SM, Doger de Spéville B, Gettinger SN, Häfliger S, Sukari A, Papa S, Rodríguez-Moreno JF, Graf Finckenstein F, Fiaz R, *et al*: Lifileucel, an autologous tumor-infiltrating lymphocyte monotherapy, in patients with advanced non-small cell lung cancer resistant to immune checkpoint inhibitors. Cancer Discov 14: 1389-1402, 2024.
4. Qu J, Mei Q, Liu L, Cheng T, Wang P, Chen L and Zhou J: The progress and challenge of anti-PD-1/PD-L1 immunotherapy in treating non-small cell lung cancer. Ther Adv Med Oncol 13: 1758835921992968, 2021.
5. Yin J, Wu Y, Yang X, Gan L and Xue J: Checkpoint inhibitor pneumonitis induced by anti-PD-1/PD-L1 therapy in non-small-cell lung cancer: Occurrence and mechanism. Front Immunol 13: 830631, 2022.
6. Rittmeyer A, Barlesi F, Waterkamp D, Park K, Ciardiello F, von Pawel J, Gadgeel SM, Hida T, Kowalski DM, Dols MC, *et al*: Atezolizumab versus docetaxel in patients with previously treated non-small-cell lung cancer (OAK): A phase 3, open-label, multicentre randomised controlled trial. Lancet 389: 255-265, 2017.
7. Zhao Z, Wang X, Qu J, Zuo W, Tang Y, Zhu H and Chen X: Immune-related adverse events associated with outcomes in patients with NSCLC treated with anti-PD-1 inhibitors: A systematic review and meta-analysis. Front Oncol 11: 708195, 2021.
8. Zhang Q, Wang W, Yuan Q, Li L, Wang YC, Chi CZ and Xu CH: Correlation between immune-related adverse events and the efficacy of PD-1/PD-L1 inhibitors in the treatment of non-small cell lung cancer: Systematic review and meta-analysis. Cancer Chemother Pharmacol 89: 1-9, 2022.
9. Xie X, Wang L, Li Y, Xu Y, Wu J, Lin X, Lin W, Mai Q, Chen Z, Zhang J, *et al*: Multi-organ immune-related adverse event is a risk factor of immune checkpoint inhibitor-associated myocarditis in cancer patients: A multi-center study. Front Immunol 13: 879900, 2022.
10. Zhou YW, Zhu YJ, Wang MN, Xie Y, Chen CY, Zhang T, Xia F, Ding ZY and Liu JY: Immune checkpoint inhibitor-associated cardiotoxicity: Current understanding on its mechanism, diagnosis and management. Front Pharmacol 10: 1350, 2019.
11. Chen X, Jiang A, Zhang R, Fu X, Liu N, Shi C, Wang J, Zheng X, Tian T, Liang X, *et al*: Immune checkpoint inhibitor-associated cardiotoxicity in solid tumors: Real-world incidence, risk factors, and prognostic analysis. Front Cardiovasc Med 9: 882167, 2022.
12. Moslehi J, Lichtman AH, Sharpe AH, Galluzzi L and Kitsis RN: Immune checkpoint inhibitor-associated myocarditis: Manifestations and mechanisms. J Clin Invest 131: e145186, 2021.
13. Chen Y, Jia Y, Liu Q, Shen Y, Zhu H, Dong X, Huang J, Lu J and Yin Q: Myocarditis related to immune checkpoint inhibitors treatment: Two case reports and literature review. Ann Palliat Med 10: 8512-8517, 2021.
14. Coustal C, Vanoverschelde J, Quantin X, Lesage C, Michot JM, Lappara A, Ederhy S, Assenat E, Faure M, Issa N, *et al*: Prognosis of immune checkpoint inhibitors-induced myocarditis: A case series. J Immunother Cancer 11: e004792, 2023.
15. Wang D, Bauersachs J and Berliner D: Immune checkpoint inhibitor associated myocarditis and cardiomyopathy: A translational review. Biology (Basel) 12: 472, 2023.
16. Jiménez-Alejandre R, Ruiz-Fernández I and Martín P: Pathophysiology of immune checkpoint inhibitor-induced myocarditis. Cancers (Basel) 14: 4494, 2022.
17. Gong J, Neilan TG and Zlotoff DA: Mediators and mechanisms of immune checkpoint inhibitor-associated myocarditis: Insights from mouse and human. Immunol Rev 318: 70-80, 2023.
18. Postow MA, Sidlow R and Hellmann MD: Immune-related adverse events associated with immune checkpoint blockade. N Engl J Med 378: 158-168, 2018.
19. Liu X, Wu W, Fang L, Liu Y and Chen W: TNF-α inhibitors and other biologic agents for the treatment of immune checkpoint inhibitor-induced myocarditis. Front Immunol 13: 922782, 2022.

20. Wang J, Zhou T, Sun Z, Ye T, Zhou S, Li J, Liu Y, Kong L, Tang J, Liu D and Xing HR: Zeb1 regulates the symmetric division of mouse lewis lung carcinoma stem cells through numb mediated by miR-31. Int J Biol Sci 14: 1399-1410, 2018.
21. National Research Council (USA): Guide for the care and use of laboratory animals, 8th edition. National Academies Press, Washington, DC, pp11-123, 2011.
22. Livak KJ and Schmittgen TD: Analysis of relative gene expression data using real-time quantitative PCR and the 2(-Delta Delta C(T)) method. Methods 25: 402-408, 2001.
23. Xu L, Chen YK, Xiong L, Shen Y, Zhou Z, Wang S and Xu X: A review of immune checkpoint inhibitor-associated myocarditis: Epidemiology, pathogenesis, and biomarkers. Hum Vaccin Immunother 21: 2512645, 2025.
24. Al-Kindi SG and Oliveira GH: Reporting of immune checkpoint inhibitor-associated myocarditis. Lancet 392: 382-383, 2018.
25. Sun Z, Shen K, Xie Y, Hu B, He P, Lu Y and Xue H: Shiquan Yuzhen Decoction inhibits angiogenesis and tumor apoptosis caused by non-small cell lung cancer and promotes immune response. Am J Transl Res 13: 7492-7507, 2021.
26. Cui Y, Luo Y, Qian Q, Tian J, Fang Z, Wang X, Zeng Y, Wu J and Li Y: Sanguinarine regulates tumor-associated macrophages to prevent lung cancer angiogenesis through the WNT/β-catenin pathway. Front Oncol 12: 732860, 2022.
27. Huang F, Cao Y, Wang C, Lan R, Wu B, Xie X, Hong J, Fu L and Wu G: PNMA5 promotes bone metastasis of non-small-cell lung cancer as a target of BMP2 signaling. Front Cell Dev Biol 9: 678931, 2021.
28. Chan YP, Chuang CH, Lee I and Yang NC: Lycopene in combination with sorafenib additively inhibits tumor metastasis in mice xenografted with lewis lung carcinoma cells. Front Nutr 9: 886988, 2022.
29. Han N, Yang ZY, Xie ZX, Xu HZ, Yu TT, Li QR, Li LG, Peng XC, Yang XX, Hu J, *et al*: Dihydroartemisinin elicits immunogenic death through ferroptosis-triggered ER stress and DNA damage for lung cancer immunotherapy. Phytomedicine 112: 154682, 2023.
30. Wang P, Fang X, Yin T, Tian H, Yu J and Teng F: Efficacy and safety of anti-PD-1 plus anlotinib in patients with advanced non-small-cell lung cancer after previous systemic treatment failure-A retrospective study. Front Oncol 11: 628124, 2021.
31. Patel RP, Parikh R, Gunturu KS, Tariq RZ, Dani SS, Ganatra S and Nohria A: Cardiotoxicity of immune checkpoint inhibitors. Curr Oncol Rep 23: 79, 2021.
32. Nishikawa T, Inoue T, Otsuka T, Kuno I, Kukita Y, Nakamura H, Ikeda Y, Yasui T, Shioyama W, Oka T, *et al*: Prevalence and characteristics of immune checkpoint inhibitor-related myocardial damage: A prospective observational study. PLoS One 17: e0275865, 2022.
33. Wu Y, Xu Y and Xu L: Drug therapy for myocarditis induced by immune checkpoint inhibitors. Front Pharmacol 14: 1161243, 2023.
34. Ali A, Caldwell R, Pina G, Beinart N, Jensen G, Yusuf SW, Koutroumpakis E, Hamzeh I, Khalaf S, Iliescu C, *et al*: Elevated IL-6 and tumor necrosis factor-α in immune checkpoint inhibitor myocarditis. Diseases 12: 88, 2024.
35. Johnson DB, Balko JM, Compton ML, Chalkias S, Gorham J, Xu Y, Hicks M, Puzanov I, Alexander MR, Bloomer TL, *et al*: Fulminant myocarditis with combination immune checkpoint blockade. N Engl J Med 375: 1749-1755, 2016.
36. Naidoo J, Cottrell TR, Lipson EJ, Forde PM, Illei PB, Yarmus LB, Voong KR, Feller-Kopman D, Lee H, Riemer J, *et al*: Chronic immune checkpoint inhibitor pneumonitis. J Immunother Cancer 8: e000840, 2020.
37. Suresh K, Naidoo J, Zhong Q, Xiong Y, Mammen J, de Flores MV, Cappelli L, Balaji A, Palmer T, Forde PM, *et al*: The alveolar immune cell landscape is dysregulated in checkpoint inhibitor pneumonitis. J Clin Invest 129: 4305-4315, 2019.
38. Yang K, Li J, Sun Z, Zhao L and Bai C: Retreatment with immune checkpoint inhibitors in solid tumors: A systematic review. Ther Adv Med Oncol 12: 1758835920975353, 2020.
39. Kim CG, Kim KH, Pyo KH, Xin CF, Hong MH, Ahn BC, Kim Y, Choi SJ, Yoon HI, Lee JG, *et al*: Hyperprogressive disease during PD-1/PD-L1 blockade in patients with non-small-cell lung cancer. Ann Oncol 30: 1104-1113, 2019.
40. Heckmann MB, Finke D, Sauerbrey L, Frey N and Lehmann LH: Increased expression of human endogenous retrovirus K in endomyocardial biopsies from patients with cardiomyopathy-a transcriptomics meta-analysis. BMC Genomics 25: 707, 2024.
41. Zhang Y, Sun X, Jin Y, Chen K, Zhang L, Gao X, Li M, Yuan Z, Jia J, Sun A and Ge J: Mitochondrial transplantation augments the reparative capacity of macrophages following myocardial injury. Adv Sci (Weinh) 12: e06337, 2025.
42. Kim H, Ahn HS, Hwang N, Huh Y, Bu S, Seo KJ, Kwon SH, Lee HK, Kim JW, Yoon BK and Fang S: Epigenomic landscape exhibits interferon signaling suppression in the patient of myocarditis after BNT162b2 vaccination. Sci Rep 13: 8926, 2023.
43. Patel T, Kelleman M, West Z, Peter A, Dove M, Butto A and Oster ME: Comparison of multisystem inflammatory syndrome in children-related myocarditis, classic viral myocarditis, and COVID-19 vaccine-related myocarditis in children. J Am Heart Assoc 11: e024393, 2022.
44. Wang X, Chen J, Shen Y, Zhang H, Xu Y, Zhang J and Cheng L: Baricitinib protects ICIs-related myocarditis by targeting JAK1/STAT3 to regulate macrophage polarization. Cytokine 179: 156620, 2024.
45. Nishikawa T, Tamiya M, Ohta-Ogo K, Ikeda Y, Hatakeyama K, Honma K, Yasui T, Shioyama W, Oka T, Inoue T, *et al*: A case of lung cancer with very-late-onset immune checkpoint inhibitor-related myocarditis. CJC Open 4: 651-655, 2022.
46. Nishikawa T, Kunimasa K, Ohta-Ogo K, Ikeda Y, Yasui T, Shioyama W, Oka T, Honma K, Hatakeyama K, Kumagai T and Fujita M: Sinus node dysfunction co-occurring with immune checkpoint inhibitor-associated myocarditis. Intern Med 61: 2161-2165, 2022.
47. Flippe L, Bézie S, Anegon I and Guillonneau C: Future prospects for CD8+ regulatory T cells in immune tolerance. Immunol Rev 292: 209-224, 2019.
48. Valaperti A, Nishii M, Liu Y, Naito K, Chan M, Zhang L, Skurk C, Schultheiss HP, Wells GA, Eriksson U and Liu PP: Innate immune interleukin-1 receptor-associated kinase 4 exacerbates viral myocarditis by reducing CCR5(+) CD11b(+) monocyte migration and impairing interferon production. Circulation 128: 1542-1554, 2013.
49. Lin W, Wang Y, Li M, Feng J, Yue Y, Yu J, Hu Y and Suo Y: Tumor treating fields enhance anti-PD therapy by improving CCL2/8 and CXCL9/CXCL10 expression through inducing immunogenic cell death in NSCLC models. BMC Cancer 25: 489, 2025.
50. Tan H, Shah NUH, He B, Liu T, Li T, Liu M, Gu Y, Zhi C, Ou Y, Huang J, *et al*: Intratumoral delivery of PD-1/PD-L1 and CTLA-4 inhibitors for recurrent/refractory solid tumors: A proof-of-concept treatment strategy. Front Immunol 16: 1669924, 2025.